

FEW MILLIMETER PRECISION FOR  
BASELINES IN THE CALIFORNIA PERMANENT GPS GEODETIC ARRAY

Ulf J. Lindqwister, James F. Zumberge, Frank H. Webb, and Geoffrey Blewitt

Jet Propulsion Laboratory, California Institute of Technology

**Abstract.** Geodetic measurements with Rogue Global Positioning System (GPS) receivers from sites in the California Permanent GPS Geodetic Array (PGGA) have been analyzed using the GIPSY orbit-determination and baseline-estimation software. Based on an unbiased selection of 23 daily measurements spanning 8 months, the low-frequency ( $\geq$  weeks) contributions to the long-term repeatabilities of baseline measurements are approximately 5, 3, and 8 mm for the east, north, and vertical components. Short-term contributions to the long-term repeatabilities were evaluated by examining data from the week of October 21, 1990, which showed the lowest short-term scatter. For this week, daily repeatabilities of 2-3 mm in the horizontal and 4 mm in the vertical have been achieved for the 172-km JPL-Pinyon baseline, consistent with carrier phase data noise of  $\sim$ 6 mm. High quality ( $\leq$  5 mm) repeatabilities have been achieved for all components of the other baselines as well.

## Introduction

A continuously monitored array of three GPS Rogue receivers was deployed in southern California in the spring of 1990. The array has since been operated jointly by the Jet Propulsion Laboratory (JPL) and Scripps Institution of Oceanography. GPS networks of this nature are capable of yielding high precision (few mm over several hours) or high temporal resolution ( $\sim$ cm over few minutes) displacement measurements over baseline lengths up to several hundred kilometers. Such networks will facilitate the use of GPS for numerous applications including mapping the strain pattern in fault zones; pre-, co-, and post-seismic fault monitoring; long-term tectonic deformation studies; monitoring of volcanic uplift; studying sea level changes; and supporting precise orbit determination of remote sensing satellites carrying GPS receivers. In addition, permanent arrays provide an opportunity to study GPS systematic error sources, such as antenna multipath, tropospheric delay mismodeling, and system noise.

In this letter, PGGA data from selected weeks in 1990 have been analyzed to obtain preliminary estimates of long-term baseline repeatabilities. The selection criteria, believed to be statistically unbiased, were essentially data availability, short-term continuity, and long-term coverage. In addition, an in-depth study of data from the week of October 21-27, 1990 is presented. The purpose here is to demonstrate the level of short-term precision which may be obtained with GPS during ideal observing conditions. For this particular week three-dimensional short-term repeatabilities at the few-millimeter level were obtained for baselines up to 170 km in length.

Copyright 1991 by the American Geophysical Union.

Paper number 91GL01289  
0094-8534/91/91GL-01289\$3.00

## Methods

The PGGA currently consists of GPS receivers located at JPL (Pasadena), Scripps Institution of Oceanography (La Jolla), and Pinyon Flat Observatory, approximately 172 km ESE of JPL (Figure 1). Each station is equipped with a Rogue SNR-8 receiver, which measures dual band P-code pseudorange and carrier phase observables, and a choke-ring backplane antenna to minimize multipath. The monuments at JPL and Pinyon Flat are collocated with Very Long Baseline Interferometry (VLBI), and hence GPS estimates for this baseline can be compared against an independent measurement technique for assessing accuracy.

For reference frame control and improved GPS orbits, data from three Cooperative International GPS Network (CIGNET) sites in North America were combined with the PGGA data. The CIGNET sites are located at Richmond (FL), Mojave (CA), and Westford (MA). Each station employs a MiniMac 2816 AT receiver, providing dual band carrier phase observables only. For both receivers all data types were decimated to 6-minute intervals. The coordinates of the CIGNET stations and the JPL site were held fixed at a priori values based on the VLBI GLB223 solution (J. Ryan, et al., Goddard Space Flight Center VLBI group, unpublished results, 1987). The Scripps and Pinyon sites were estimated as constants as were all satellite state parameters and carrier phase biases. Clocks were estimated as white process noise and all the a priori sigmas were left unconstrained [Lindqwister et al., 1990].

The tropospheric path delays may be subdivided into a dry (hydrostatic) and a wet delay. The dry delay is typically very stable and a nominal offset of 2 m was removed. The total wet delay and the residual dry delay were estimated using a zenith bias parameter and the Lanyi wet mapping function [Lanyi, 1984]. For the October data set low-angle mismodeling was studied by varying the low elevation cutoff angle as described below. The wet delay varies considerably

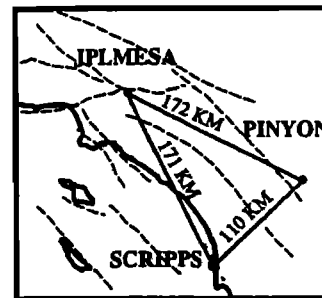


Fig. 1. The California PGGA sites are shown in relation to nearby faults (dashed lines).

over a day and was estimated stochastically by using a random walk stochastic model [Lichten, 1990]. The random walk model is characterized by the time derivative of its variance, set here to  $(6 \text{ cm day}^{-1/2})^2$ .

The analysis of data from the PGGA and CIGNET sites was performed with the GIPSY orbit determination and baseline estimation software [Lichten, 1990]. The two data streams are processed separately, because of different analysis paths. The Rogue data are edited with Turboedit [Blewitt, 1990], which relies on dual band P-code pseudorange and carrier phase observables to perform robust carrier cycle repair after losses of lock. Because the MiniMac has no P-code capability, a codeless algorithm has been developed which single differences data between CIGNET receivers to eliminate satellite clock offsets and effects of Selective Availability. A station location and satellite model is subtracted from the differenced data, thus producing a smooth residual, which is input to a Kalman filter. If discontinuities are found by the filter, then the receiver with the cycle slip may easily be determined by comparing the residuals in each of three differenced files. The correction is finally applied to the undifferenced data. Alternatively, an extra phase ambiguity parameter is introduced if the cycle-slip cannot be resolved.

Simultaneous processing of the Rogue and MiniMac data is theoretically better since it increases satellite mutual visibility. However, this would require careful treatment of antenna phase variations between the different antenna types used in CIGNET and the PGGA. Parameter estimation is performed separately for the PGGA and CIGNET networks. To combine information (estimates and covariances) from each network, a weighted method is used. If  $x_1$  and  $x_2$  are independent estimates with covariances  $P_1$  and  $P_2$ , the combined estimate is

$$\mathbf{x} = \mathbf{P} (\mathbf{P}_1^{-1} \mathbf{x}_1 + \mathbf{P}_2^{-1} \mathbf{x}_2), \quad (1)$$

where  $\mathbf{P} = (\mathbf{P}_1^{-1} + \mathbf{P}_2^{-1})^{-1}$  is the combined covariance.

The orbital information (satellite position, velocity, and solar radiation pressure coefficients) from the CIGNET solution is extracted and combined with the corresponding solution from the PGGA sites using an algorithm which effectively implements (1) [e.g. Bierman, 1977]. The resulting Rogue solutions are considerably improved with the addition of the wider aperture continental orbital data. For the California PGGA over 90% of all the carrier phase biases were resolved, with a cumulative confidence limit of 99%. For the seven single-day solutions obtained with data from October 21-27, 1990, ambiguity resolution resulted on average in a factor of 3.6, 1.5, and 1.1 improvement in the daily repeatabilities in the east, north, and vertical components for all three baselines, which is consistent with previous applications of ambiguity resolution in California [Blewitt, 1989]. Note that the PGGA carrier phase biases could not be resolved without orbital enhancement from the CIGNET data.

#### Results

##### Long-term Repeatability

Shown in Figure 2 are the results of the analysis for the Pinyon-to-JPL baseline for a period spanning ~8 months.

Each plotted point corresponds to a single-day solution with a parameter-estimation strategy essentially identical to that used in producing the results presented in detail below for the week of October 21. The vertical bar accompanying each point reflects the formal error. The area between the dotted lines in Figure 2 is the plus-or-minus one standard deviation region defined by rates from the VLBI solution GLB659 [Caprette et al., 1990], with an offset adjusted to minimize the weighted mean-square difference from the PGGA results. The offsets were 21 mm east, -22 mm north, and 24 mm vertical. These biases may be due to unknown VLBI-GPS phase center offsets and ground tie errors.

It is clear from the figure that the short-term scatter of the PGGA results is often considerably less than the long-term scatter. A simple model for the error in the measurement of a baseline component [Davis et al., 1989] is

$$e = \sigma \delta_1 + s \delta_2, \quad (2)$$

where  $\sigma$  scales the low-frequency ( $\geq$ weeks) errors and  $s$  scales the short-term errors. In (2),  $\delta_1$  and  $\delta_2$  are independent random variables with zero mean and unit variance.  $\delta_1$  is a slowly-varying quantity, while  $\delta_2$  is essentially white noise. The long-term repeatability will be  $(\sigma^2 + s^2)^{1/2}$ .

The data in Figure 2 can be divided naturally into five groups, with each group containing two or more consecutive or nearly-consecutive daily measurements. The short-term repeatability  $s_i$  can be estimated empirically for the  $i^{\text{th}}$  group as the standard deviation of the measurements in the group. To estimate the low-frequency component  $\sigma$ , we use the likelihood function

$$L(\sigma) \propto \prod_{i=1}^5 \frac{1}{\sqrt{2\pi(\sigma^2 + S_i^2)}} \exp \left[ -\frac{\delta x_i^2}{2(\sigma^2 + S_i^2)} \right] \quad (3)$$

to indicate the level at which the data are consistent with a given value of  $\sigma$ . In (3),  $S_i$  is the uncertainty in the average of the  $i^{\text{th}}$  group ( $= s_i$  divided by the square-root of the number of days in the group) and  $\delta x_i$  is deviation of the  $i^{\text{th}}$  average from the weighted average of all points. (The results are largely insensitive to reasonable a priori assumptions of rate.) The value of  $\sigma$  which maximizes  $L(\sigma)$  is the maximum likelihood estimate (MLE) of the true value of  $\sigma$  [e.g., Mathews and Walker, 1970]. The results are summarized in Table 1 for all baselines in the array. The quoted lower (upper) number, when added to the MLE, is the value of  $\sigma$  below (above) which the integral of  $L(\sigma)$  is 15.87% of its value from 0 to  $\infty$ . In those instances where the MLE is zero, we quote only the 84.13%-confidence upper limit.

The PGGA data in Figure 2 are not inconsistent with the rates from the VLBI GLB659 solution. However, because

Table 1 Low-frequency Errors  $\sigma$  (millimeters)

Baseline	East	North	Vertical
Pinyon to JPL (172 km)	5.6 <sup>+5.8</sup> <sub>-1.0</sub>	< 1.9	8.5 <sup>+9.2</sup> <sub>-2.5</sub>
Scripps to JPL (171 km)	5.2 <sup>+5.1</sup> <sub>-0.8</sub>	2.7 <sup>+3.3</sup> <sub>-0.5</sub>	< 5.4
Scripps to Pinyon (111 km)	< 2.9	3.4 <sup>+3.7</sup> <sub>-0.7</sub>	8.3 <sup>+9.8</sup> <sub>-2.0</sub>

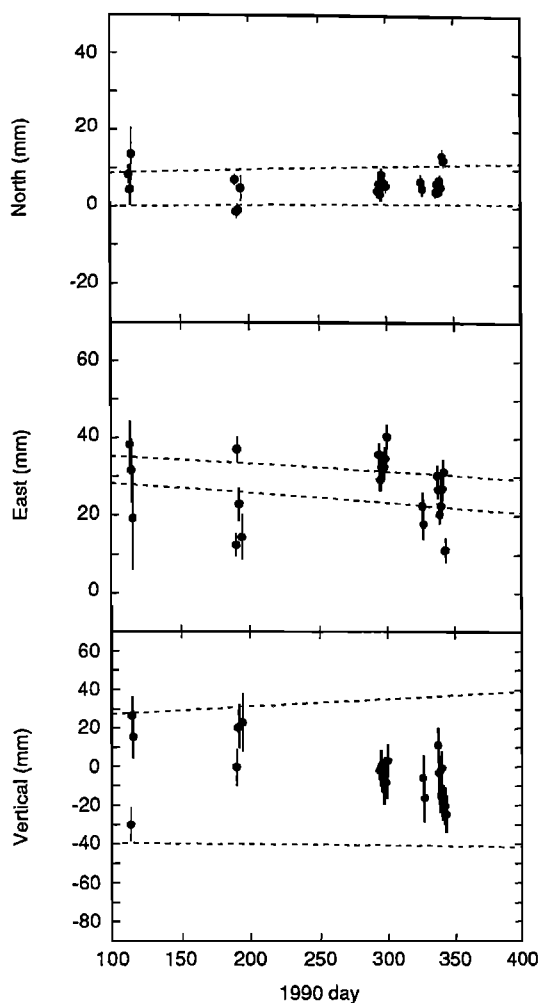


Fig. 2. Long-term repeatability for the Pinyon-to-JPL baseline. The region enclosed by the dotted lines indicates the VLBLI solution GLB659 extrapolated to 1990.

their low-frequency errors are significant, estimates of baseline rates in this array would be premature at this time. The results are nevertheless valuable in that they imply specific observation times required to measure a given rate at some level of significance. If one assumes that multi-day averaging can effectively eliminate the short-term errors, and that the low-frequency errors become uncorrelated over some time  $\tau$ , then to measure a rate  $R$  to within  $\pm\sigma_R$  would require a period

$$T = \left( \frac{12\sigma^2\tau}{\sigma_R^2} \right)^{1/3} \quad (4)$$

(the expression assumes uniform distribution of the measurements over  $T$ ). With  $\tau = 1$  month, for example, the east component of the Pinyon-to-JPL rate could be measured to an accuracy of 2 mm/yr (or signal to noise of about 4 to 1, given the  $\sim 8$ -mm/yr rate from GLB659) in  $T = 2$  years.

#### Daily Repeatabilities and Formal Errors

The week of October 21 (7 days) provided ideal observing conditions for GPS. Satellite eclipsing was altogether absent

for this week. Eclipsing occurs when the GPS satellite moves in and out of the shadow of the earth, each time experiencing an impulse force due to the change in the solar radiation pressure, which is currently not modeled correctly. The daily repeatabilities for all baseline components from this week are summarized in Table 2. The day-by-day results for the JPL-Pinyon baseline are plotted in Figure 3. An earlier high precision GPS study showed similar few-mm horizontal repeatabilities for 200-700-km baselines [Lindqwister et al., 1990]. In the current study, however, the vertical repeatabilities have improved by a factor of  $\sim 3$  and are now at the half-centimeter level. The improvement is most likely due to better satellite coverage and the use of 8 channel, low multipath receivers (Rogue), as compared to the 4 channel TI-4100 receivers employed in the previous study.

The formal error bars drawn in Figure 3 account for data noise, the geometric strength of the satellite configuration, and the number of measurements. To assess the consistency of the observed daily repeatabilities with the formal errors, we show in Figure 4 a plot of the former vs. the latter. Four components (east, north, vertical, and length) from each of the three baselines are shown. The asymmetry of the vertical error bars arise from the asymmetric  $\chi^2$  distribution, which describes the degree to which an rms can be estimated from only 7 measurements. The magnitude of the data noise, to which formal errors scale, has been set to 6.3 mm, giving a slope of  $\sim 1$  in Figure 4. The observed fluctuations in the vertical are slightly lower than would be expected from the results of the other components. The 6.3-mm data noise also agrees with the post-fit residuals for the carrier phase observable. For example, the 12-hour estimated standard deviation of the carrier phase noise based on post-fit residuals for the CIGNET sites averaged 6 mm on October 25. Similarly for the PPGA sites on October 21 the residuals averaged 4-5 mm.

#### Sensitivity of Baseline Estimates to Estimation Strategy

The nominal estimation strategy combines CIGNET and PPGA solutions, cuts off low-elevation-angle data, and treats the troposphere as a random walk (RW). Many variations of this strategy are of course possible. For example, by using only the first four or last three days of CIGNET data to provide orbital data for the entire week, it was found that baseline solutions varied at the level of 1-5 mm for all three baselines in all components. In addition, the troposphere stochastic model was changed from a random walk to a first-order Gauss-Markov (GM) process. With steady-state sigmas of 6-12 mm and time constants of 0.5-3.4 hrs the baseline estimates were virtually unchanged. However, comparing GM and RW stochastic models revealed differences in the

Table 2 Daily Repeatabilities (millimeters)

Baseline	East	North	Vertical
Pinyon to JPL (172 km)	3.4	1.6	4.1
Scripps to JPL (171 km)	2.5	2.0	5.3
Scripps to Pinyon (111 km)	1.6	1.6	7.7

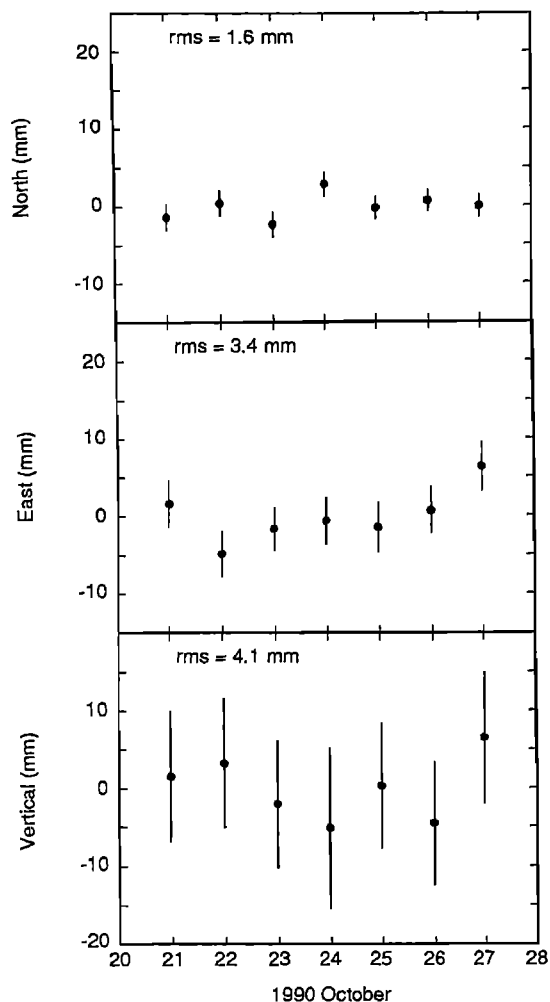


Fig. 3. Daily results for the Pinyon-to-JPL (172-km) baseline, with each component adjusted to zero mean. The rms scatter is 2-4 mm for all components.

vertical estimate of  $\sim 15$  mm. Variations in the elevation cutoff angle were also studied. As the cutoff angle was lowered and more data were added, all baseline repeatabilities improved, consistent with what would be expected from formal errors. Below  $15^\circ$  (our optimal value), however, the daily repeatabilities started increasing, deviating

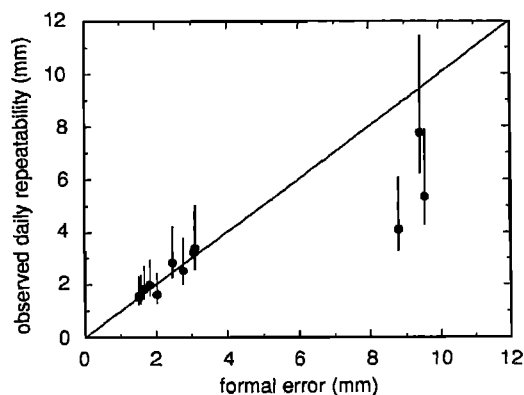


Fig. 4. A comparison of daily repeatability with formal errors.

from the formal-error prediction, thus indicating some low-angle mismodeling.

### Conclusions

Based on 23 daily measurements spanning 8 months, the long-term repeatabilities of baseline measurements in the PPGA are less than or approximately equal to 6 mm in the horizontal and 10 mm in the vertical. The high-precision GPS analysis indicates that in the short-term (one week) precision at the few-millimeter level is achievable in all baseline components, including the vertical, for baselines up to 170 km in length, with post-fit residuals that are consistent with the formal errors. These results are based on data from the PPGA, using 8-channel Rogue receivers equipped with low multipath antennas. Orbit enhancement for the regional data was accomplished by combining the PPGA solutions with information from solutions based on CIGNET data.

*Acknowledgments.* The authors appreciate discussions with S. Lichten, K. Hurst, R. Treuhaft, and T. Yunck and would also like to thank two anonymous reviewers for helpful comments. The work described in this letter was carried out by the Jet Propulsion Laboratory, California Institute of Technology, under contract with the National Aeronautics and Space Administration.

### References

- Bierman, G. J., *Factorization Methods for Discrete Sequential Estimation*, V128, Mathematics in Science and Engineering Series, Academic Press, 1977.
- Blewitt, G., Carrier phase ambiguity resolution for the global positioning system applied to geodetic baselines up to 2000 km, *JGR*, 94, 10187-10203, 1989.
- Blewitt, G., An Automatic Editing Algorithm for GPS data *GRL*, 17, No. 3, pp. 199-202, March 1990.
- Caprette, D. S., C. Ma, and J. W. Ryan, "Crustal Dynamics Project Data Analysis--1990", VLBI Geodetic Results 1979-1989, NASA TM 100765, December, 1990.
- Davis, J. L., W. H. Prescott, J. L. Svarc, and K. J. Wendt, "Assessment of Global Positioning System Measurements for Studies of Crustal Deformation", *JGR*, 94, 13635, 1989.
- Lanyi, G., Tropospheric Calibration in Radio Interferometry, *Proc. Int. Symp. Space Tech. Geodyn., IAG COSPAR*, 2, p.184, 1984.
- Lichten, S., Estimation and filtering for high-precision GPS positioning applications, *Man. Geod.*, 15, 159-176, 1990.
- Lindqwister, U.J., S. M., Lichten, and G. Blewitt, Precise regional baseline estimation using a priori orbital information, *GRL*, 17, No. 3, pp. 219-222, March 1990.
- Mathews, J., and R. L. Walker, *Mathematical Methods of Physics*, 2nd Ed, 501 pp., W. Benjamin, Menlo Park, 1970.
- G. Blewitt, U. Lindqwister, F. Webb, and J. Zumbege, Mail-Stop: 238-625, Jet Propulsion Laboratory, Pasadena, CA 91109.

(Received January 25, 1991;  
revised April 8, 1991;  
accepted April 25, 1991.)